

The mechanism of protection zone expansion in protected seam with a large-spaced lower protective seam

Cheng Xia

Anhui Energy Technology School, Hefei 230011, China.

ABSTRACT

Pansan mine employs protective mining method. The #11-2 coal seam in the mine, which lies about 70 m below the gassy and outburst-prone #13-1 seam, is mined prior to the extraction of the #13-1 seam. An investigation has been undertaken in the mine to understand the mechanism of the protection zone expansion in the #13-1 seam with the extraction of the #11-2 seam. The evolution of the stress, seam permeability and deformation in the protected coal seam was investigated with field tests and numerical modelling. The investigation results show that there exist five zones in the protected coal seam during the protective seam mining: unaffected zone, stress rising zone, minor-reducing stress zone, major-reducing stress zone, and compression zone. The results also show that the permeability increased 30 times in the minor-reducing stress zone due to stress reduction and swelling deformation. With the existence of the minor-reducing stress zone, in combination of intensive borehole drilling, the protection zone in the protected seam could be expanded.

Key words: Protective seam mining, numerical simulation, protection zone

Date of Submission: 14-01-2020

Date of acceptance: 31-01-2020

I. INTRODUCTION

Protective coal seam mining is one of the most effective methods used in managing the risk of the outbursts of coal and gas. Shi and Tu^[1-4] studied the stress relief range, swelling deformation, stress distribution and permeability change in the process of lower protective coal seam mining with both numerical and physical simulations. Yang et al.^[5] studied the mechanism of de-stressed gas flow in the process of protective coal seam mining by applying coupled damage-permeability evolution equation. Cheng et al.^[6], Yu et al.^[7], Yuan^[8-15] Hu^[16], Xue^[17], Tian^[18], Lu^[19], Hu^[20] and Li^[21] studied the safe and highly efficient integrated coal mining and long-distance stress relief gas extraction, the movement characteristics of upper long-distance de-stressed strata and related gas extraction technology, the de-stressed gas extraction technology and gas emission laws in the protected coal seam, the integrated coal mining and de-stressed gas extraction in highly gassy and super thick coal seam, and the gas extraction theory and technology in soft and low-permeability multiple seams.

However, there is little information available in the open literature about the systematical study on the protected zone expansion in the protected coal seam, and mechanical mechanism of the protected coal seam in the process of long-distance protective coal seam mining in nearly horizontal coal seams. This paper describes the investigation undertaken in Pansan mine to understand the evolution of the stress, seam permeability and deformation in the protected coal seam with field tests and numerical modelling, and presents the results of this investigation in terms of the mechanism of the protection zone expansion with the advance of protective seam mining.

II. STRESS-DAMAGE-FLOW COUPLING MODEL IN GASSY ROCK/COAL

Gas seepage field equation is as follows:

$$\alpha_p \nabla^2 (\lambda_i \cdot P) = \frac{\partial P}{\partial t} \quad (1)$$

Where, P is the square of seepage field pressure in MPa with $P = p^2$; $\alpha_p = 4\lambda A^{-1} P^{0.75}$, where, A is the gas

content coefficient in $\text{m}^3/(\text{m}^3 \cdot \text{MPa}^{0.5})$; λ is the permeability coefficient in $\text{m}^2/(\text{MPa} \cdot \text{d})$.

Constitutive equation:

$$\lambda \delta_{i,j} \varepsilon_{i,j} + 2G \varepsilon_{i,j} + (\alpha p \delta_{ij})_{,j} + f_i = 0 \quad (2)$$

Where, f_i is the body force component in MPa; α is the pore pressure coefficient with $0 < \alpha < 1$; p is the gas pressure in MPa; δ_{ij} is the Kronecker function; $\varepsilon_{i,j}$ is the strain component; λ, G are the shear modulus and Lamé constant, respectively.

Geometrical equation is:

$$\varepsilon_{i,j} = \frac{1}{2}(\mu_{i,j} + \mu_{j,i}) \quad (3)$$

Where, u is the deformation displacement.

Elastic modulus of the damaged unit can be calculated as:

$$E = (1 - D)E_0 \quad (4)$$

Where, D is the damage variant; E, E_0 are the elastic modulus of damaged and undamaged units, respectively.

Unit failure criterion is:

$$\text{When } \sigma_1 - \sigma_3 \frac{1 + \sin \phi}{1 - \sin \phi} \geq f_c, D = \begin{cases} 0 & \varepsilon < \varepsilon_{c0} \\ 1 - \frac{f_{cr}}{E_0 \varepsilon} & \varepsilon < \varepsilon_{c0} \end{cases}$$

Where, ϕ is the interior fraction angle; f_c is the uniaxial compression strength; f_{cr} is the residual uniaxial compression strength; ε_{c0} is the maximum compression strain.

Then the permeability coefficient is:

$$\lambda = \begin{cases} \lambda_0 e^{-\beta(\sigma_1 - \alpha p)} & D = 0 \\ \xi \lambda_0 e^{-\beta(\sigma_1 - \alpha p)} & D > 0 \end{cases} \quad (5)$$

Where, λ_0 is the initial gas permeability; ξ is the increase ratio of gas permeability; α is the pore pressure coefficient; β is the coupling coefficient.

$$\text{When unit tensile strength satisfies the equation: } \sigma_3 \leq -f_t, D = \begin{cases} 0 & \varepsilon > \varepsilon_{t0} \\ 1 - \frac{f_{tr}}{E_0 \varepsilon} & \varepsilon_{tu} \leq \varepsilon < \varepsilon_{t0} \\ 1 & \varepsilon \leq \varepsilon_{tu} \end{cases}$$

$$\text{Then the permeability coefficient is } \lambda = \begin{cases} \lambda_0 e^{-\beta(\sigma_3 - \alpha p)} & D = 0 \\ \xi \lambda_0 e^{-\beta(\sigma_3 - \alpha p)} & 0 < D < 1 \\ \xi' \lambda_0 e^{-\beta(\sigma_3 - \alpha p)} & D = 1 \end{cases} \quad (6)$$

Where, f_{tr} is the residual uniaxial tensile strength; ξ' is the increase coefficient of gas permeability (when the element is totally damaged).

The damage equation of mesoscopic unit of coal body under uniaxial compression and uniaxial tension is illustrated in Figure 1. The solid-gas damage coupled model is composed of Eq. (1), Eq. (2), Eq (5) and Eq. (6), and the calculating process is shown in Figure 2.

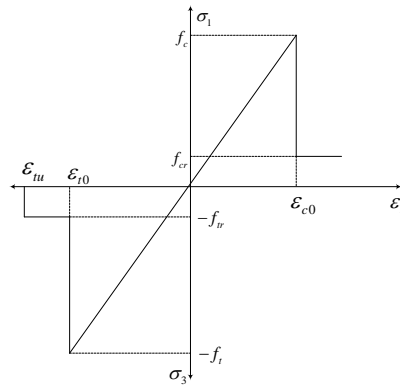


Fig. 1. Uniaxial compression and tension model

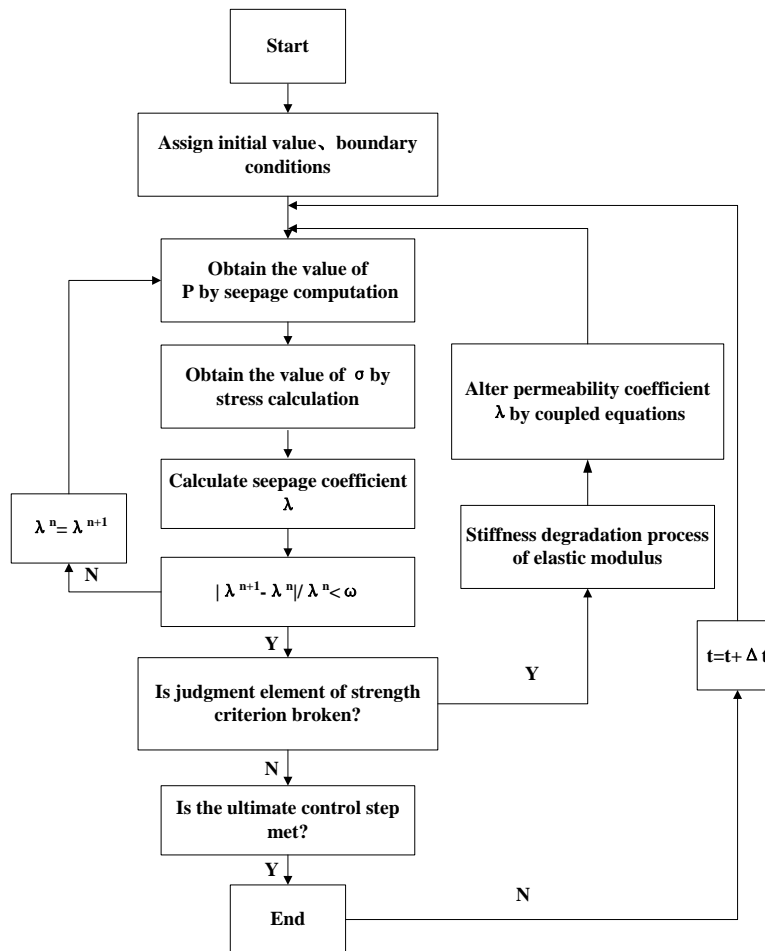


Fig. 2. Flow chart of the model

III. FIELD TESTS AND NUMERICAL MODELLING

3.1 Field test plan

The field test was conducted in Pansan coal mine, Huainan Mining Group Co. Ltd. The #11-2 seam is the protective seam and its overlying #13-1 seam is the protected seam. The 13-1 seam is about 72 m above the #11-2 seam. The test site was in longwall panel 17171(1) of 1200 m long and 190 m wide. The overburden depth of the panel was between -722m and -752m and the #11-2 seam is 2 m thick and dips about 5° . The #13-1 seam has the original gas content of between $12 \text{ m}^3/\text{t}$ and $22 \text{ m}^3/\text{t}$, the gas pressure of 3.5 MPa the dip angle of 6° and the original permeability of $2 \times 10^{-4} \text{ m}^2/\text{MPa}^2 \cdot \text{d}$. The measuring points of the field test is shown in Figure 3. The gas pressure, extraction radius and swelling deformation in the #13-1 seam were measured in the region of the #13-1 seam vertically above the start-up, haulage and rail roadways of the 17171(1) panel.

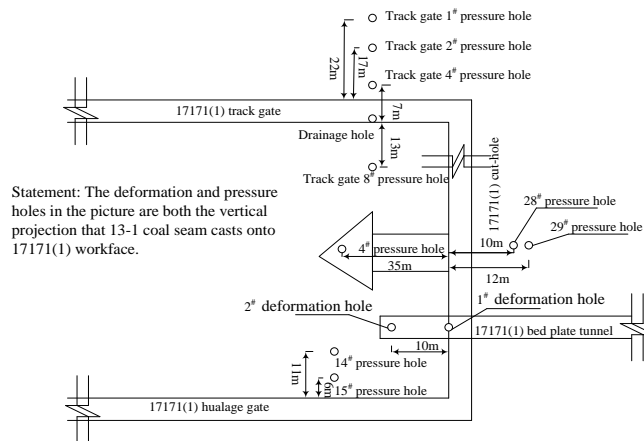


Fig. 3. The layout of the measurement points in the #13

3.2 Numerical model

The numerical model is constructed according to the gas and geological information of Pansan coal mine, as shown in Figure 4. The rock/coal mechanical parameters used in the model are listed in Table 1. The horizontal length and vertical width of the model was 300 m and 120 m, respectively, and it was divided into 120×300 units. The 10MPa pressure loaded on the model top surface was to simulate the gravity of the upper strata. The left, right and low boundaries of the model were all displacement restraint boundaries. The stratigraphic column of Pansan coal mine was pre-built in the model. The 11-2 seam was extracted with the single pass and full-height longwall mining method with an advance rate of 5 m per day.

The stress, subsidence and permeability coefficient of the model was measured in the intermediate cross-section of the #13-1 seam (profile A-A in Figure 4). The deformation of the #13-1 seam was the difference between its roof deformation and its floor deformation. Because the strata above the protective seam can be viewed as combined strata in the f protective seam mining, the trend of stress distribution along the strike and inclination of the panel was similar, therefore the numerical simulation was proceeded only along the strike.

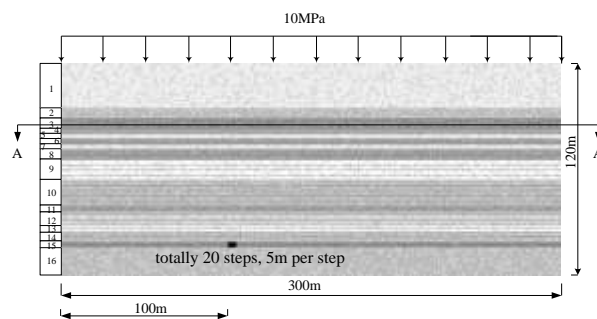


Fig. 4. Numerical model

Table 1: Mechanical parameters of coal seams and rock strata

No.	Lithology	Elastic Modulus (MPa)	Compression Strength (MPa)	Density ($10^{-5}N \cdot mm^{-3}$)	Thickness (m)
1	siltstone	57.22	63.0	2.6	26
2	sandy mudstone	37.47	37.3	2.4	6
3	coal seam #13-1	10	15.0	1.4	6
4	sandy mudstone	26	33.3	2.4	3
5	siltstone	57.23	50.3	2.6	3
6	mudstone	20	25.0	2.4	3
7	siltstone	57.23	50.3	2.6	3
8	mudstone	20	25.0	2.4	6
9	sandstone	64.55	76.3	2.6	12
10	sandy mudstone	37.47	37.3	2.4	15
11	mudstone	20	25.0	2.4	3
12	fine sandstone	47.23	50.3	2.6	8
13	sandstone	64.49	61.6	2.6	4
14	sandy mudstone	37.47	37.3	2.4	6
15	coal seam #11-2	10	20.0	1.4	2
16	sandy mudstone	37.47	37.3	2.4	14

3.3 Stress distribution characteristics

Figure 5 and Figure 7 show the numerical modelling results. It can be seen from the results that with the advance of the 1717(1) panel the upper strata of the # 11-2 seam continuously collapsed and formed a caving zone, a fracture zone and bending subsidence zone in the vertical direction. Meanwhile, five zones were formed horizontally in the protected coal seam along the panel length. These zones include the unaffected zone, stress rising zone, minor-reducing stress zone, major-reducing stress zone, and compression zone. When the #11-2 was mined 100 m, the vertical height of the caving zone and fracture zone was about 15 m and 35 m respectively, which were consistent with the field test results. Meanwhile in the protected coal seam, the length of the stress rising zone was about 80 m, the minor-reducing stress zone about 20 m, the major-reducing stress zone about 15 m, and the compression zone about 30 m. It is shown in Figure 6 that the maximum principal stress and shear stress in the #13-1 seam began to decrease and the de-stressed area started to increase with the panel advance. When the panel face was advanced to 75 m, the maximum principal stress and shear stress in the central part of the #13-1 seam (right above the goaf of the #11-2 seam) began to rebound; when the face was at 100 m, the central part began to compress, indicating that the stress relief began to decrease. Within the minor- reducing stress zone (initial swelling), major- reducing zone (swelling increasing) and compression zone of the protected seam, the maximum principal stress and shear stress were distributed in ‘W’ shape.

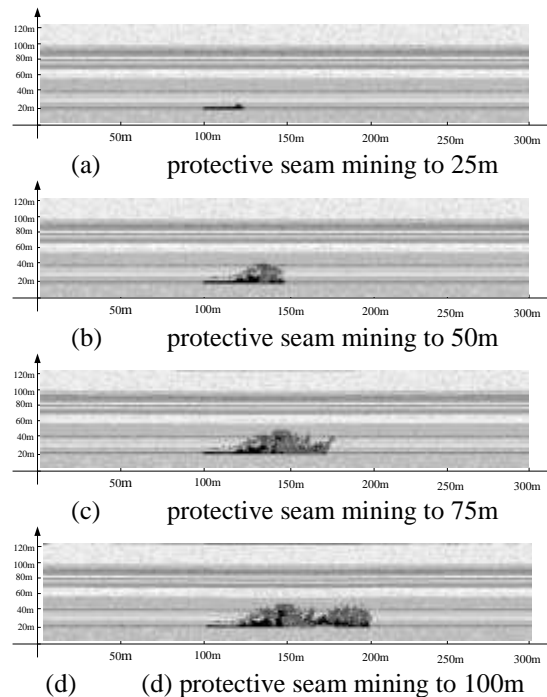


Fig. 5. The process of numerically simulated strata caving

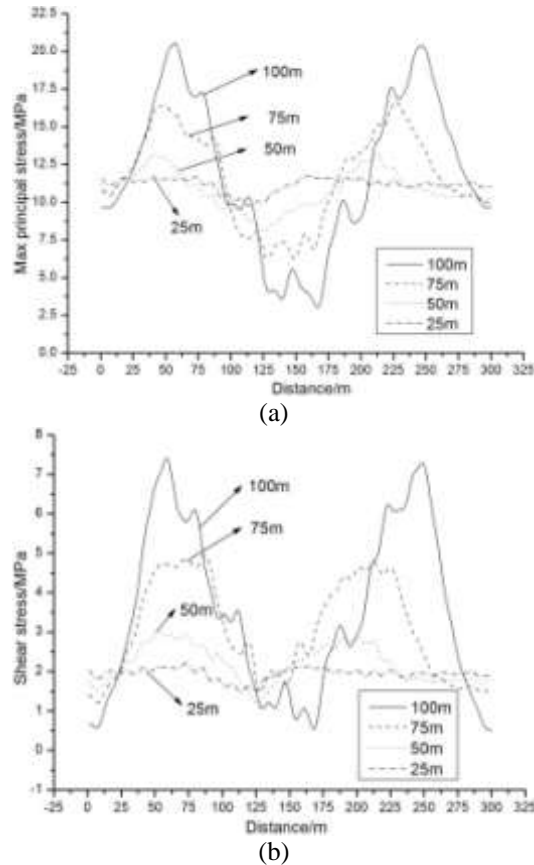


Fig. 6. The stress distribution in the #13-1 seam

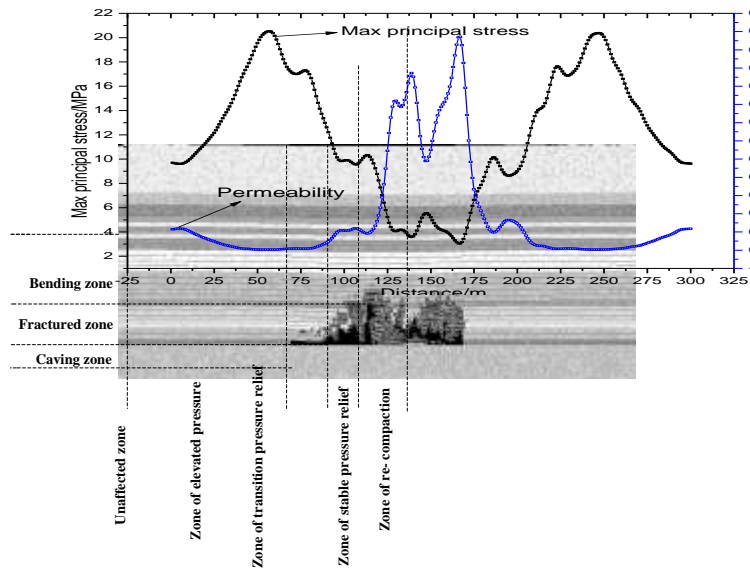
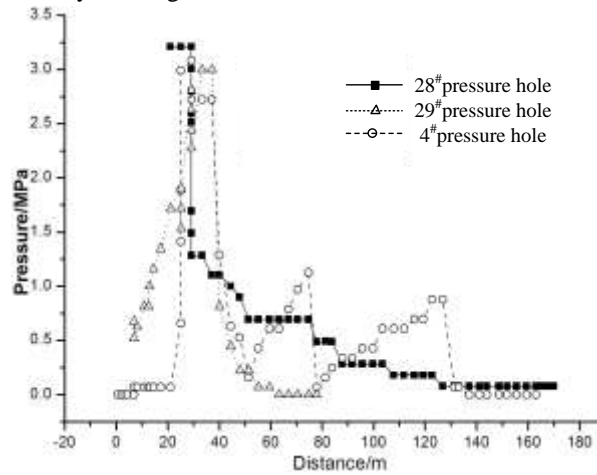


Fig. 7. Different zones in the #13-1 seam based on stress and permeability

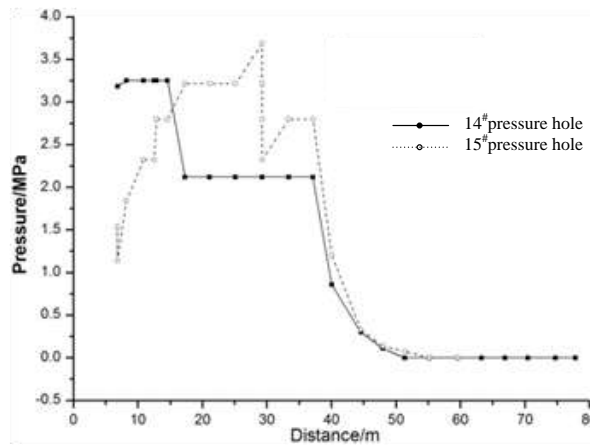
Gas pressure measuring boreholes No.28, No.29, No.4, No.14 and No.15 are shown in Figure 3. Borehole No.4 intersected between the theoretical protective line recommended in the Chinese Regulation and coal seam 13-1. The gas pressure in boreholes No.28 and No.29 continuously decreased but the degree of the reduction was smaller than that in borehole No.4 (shown in Figure 8(a) and Figure 8(b)), indicating that the stress in the major-reducing stress zone decreased more than that in the minor-reducing zone. The gas pressure in boreholes No.14 and No.15 continuously decreased in the process of protective seam mining, indicating that borehole No.14 and No.15 was within the stress reducing zone. This is consistent with numerical simulation.

The gas pressure measuring boreholes No.1 and No.2 are shown in Figure 3. The pressure in these

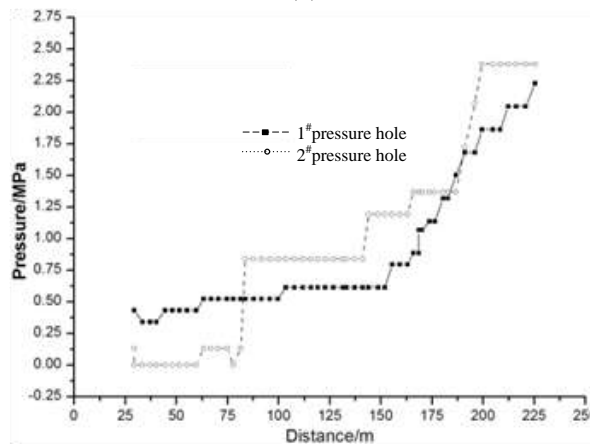
boreholes continuously increased in the process of protective seam mining, indicating that there existed a stress rising zone outside the rail roadway. This again was consistent with the numerical simulation results.



(a)



(b)



(c)

Fig. 8. The measured value of gas pressure in coal seam 13-1 induced by mining

3.4 Permeability and deformation distribution characteristics

The permeability and its distribution of the protected coal seam were greatly changed during the protective coal seam mining (shown in Figure 9). When the protective seam was mined to 100 m, the permeability was enhanced by 600 times assuming the coupling coefficient β of 1.0 and the maximum permeability coefficient of $0.12 \text{ m}^2/\text{MPa}^2 \cdot \text{d}$. The high-permeability section was in the major-reducing stress zone. In the compression zone the permeability coefficient was slightly smaller to some extent but still maintained at a

relative high level. This high-permeability section was about 60 m wide, and this is consistent with the ‘O’-shape ring theory. The permeability in the minor-reducing stress zone increased to about 30 times of the original permeability.

The swelling deformation in the protected seam increased with the advance of the protective seam mining. When the protective seam was mined to 100 m, the maximum deformation of coal seam 13-1 was about 225 mm (Figure 10). In the compression zone, the swelling deformation decreased slightly but still maintained at a relative high level due to the drop of the maximum principle stress, which was on par with the distribution of permeability coefficient.

Figs 9 and 10 indicate that permeability coefficient and swelling deformation of the protected seam were distributed in ‘M’ shape, similar to the ‘W’ shape in the minor-reducing stress zone, the major-reducing stress zone and compression zone.

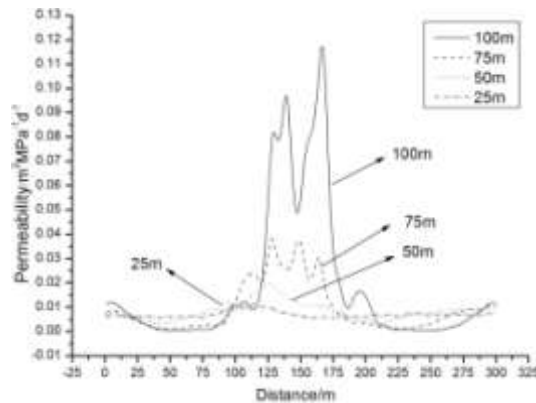


Fig. 9. Gas permeability changes induced by mining

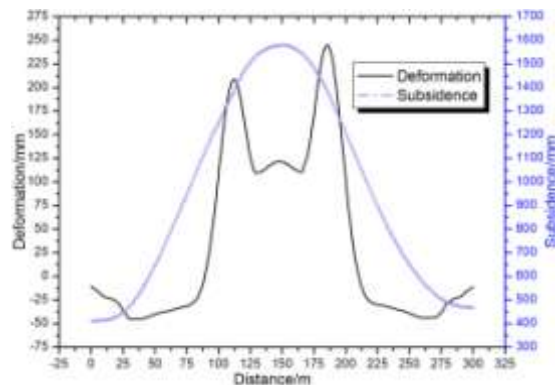


Fig. 10. Swelling deformation of coal seam 13-1 by mining

The boreholes No.4 and No.8 were shown in Figure 3 and a gas extraction borehole was arranged in the middle of these two boreholes. It is shown in Figure 11 that the effect of gas extraction within 7 m outward from the extraction radius was less than that 13 m inward from the extraction radius, indicating that permeability coefficient increased from outside to inside (shown in figure 6).

The deformation measuring borehole is shown in Figure 12. The results indicate that near the position of coal seam 13-1 vertically upper the open-off cut of coal seam 11-2, the swelling deformation was 135 mm when the protective seam was mined 100 m, which was approximately coincident to 120 mm deformation in numerical simulation.

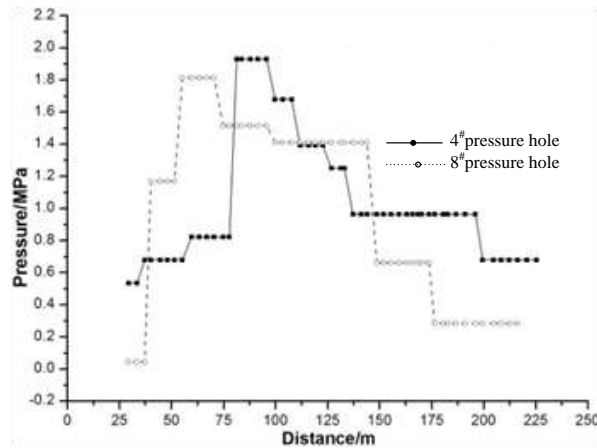


Fig. 11. Gas pressure variation in the borehole

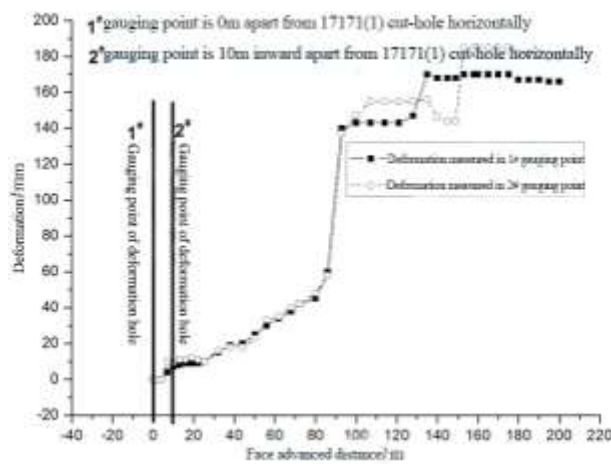


Fig. 12. Deformation between #13-1 seam roof and floor

3.5 Expansion of the protected zone

In the process of protective seam mining in DONG'SI district of PANSAN coal mine, there exists two kinds of expanding protected zone in the strata upper the open-off cut, rail entry and haulage entry (figure 13). One can be expanded to the junction between minor pressure reducing zone and major pressure reducing zone through expanding the protected zone set by Regulation; the other can be expanded to the same length and same width as the protective seam through expanding the protected zone set by Regulation. Within the range of vertically projecting the protective seam to the protected one, because of the existence of major pressure reducing zone and minor pressure reducing zone, the effect of pressure relief in the protected seam can satisfy the requirement of gas extraction. That is to say, the angle of pressure relief can be expanded from acute angle to right angle in nearly horizontal coal seam and gentle inclined coal seam. When the technique of intensive boreholes is applied in the expanding protected zone, the density of boreholes in steady expanding protected zone should be less than that in the measures-taken expanding protected zone.

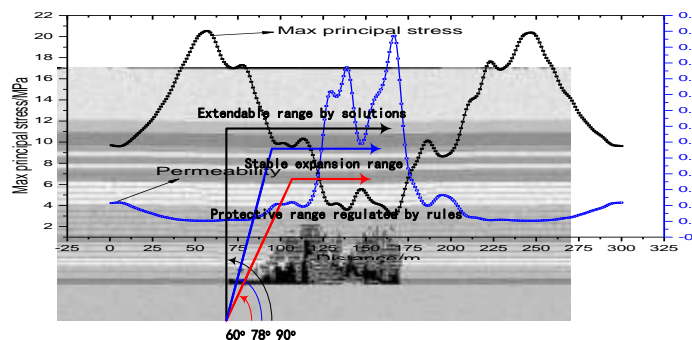


Fig. 13. Expansion of protected zone in coal seam 13-1

IV. CONCLUSIONS

In the process of protective coal seam mining, there exist five zones: unaffected zone (original stress zone), stress rising zone, minor-reducing stress zone, major-reducing stress zone, and compression zone. The permeability coefficient and swelling deformation of the protected seam were of an 'M' shape distribution, which is consistent with the 'W' shape distribution of stress in the-minor reducing stress zone, major-reducing stress zone, and compression zone. The pure existence of the minor-reducing stress zone makes the stress relief effect in the expanding protected zone of the protected seam satisfy the requirement of gas extraction. As long as the number of gas extraction boreholes is drilled and sufficient drainage time is allowed, the risk of coal and gas outburst in the expanded protected zone can be eliminated.

ACKNOWLEDGMENTS

First of all, I would like to extend my sincere gratitude to my supervisor, Yuan Liang, academician of China Engineering Academy, for his constant encouragement and guidance. Second, I would like to express my heartfelt gratitude to Professor Xue Sheng. He has walked me through all the stages of the writing of this thesis. Without his consistent and illuminating instruction, this thesis could not have reached its present form.

REFERENCES

- [1] Shi Biming, Yu Qixiang. Test and research on coal and rock movement deformation characteristics in coal mining with long distance protection layer[J]. *Coal Science & Technology*, 2005, 33(2): 39-45.
- [2] Shi Biming, Liu Zegong. Numerical simulation of the upper coal and rock deformation characteristic caused by mining protecting stratum[J]. *Journal of China Coal Society*, 2008, 33(1): 17-22.
- [3] Shi Biming. Research on the laws of the penetrability change and the coal seam deformation by the far-distance protecting stratum mining [Ph.D. Thesis] [D]. Xuzhou: China University of Mining and Technology, 2004. (in Chinese).
- [4] Tu Min, MIAO Xiexing, HUANG aibin. Deformation rule of protected coal seam exploited by using the long-distance-lower protective seam method[J]. *Journal of Mining and Safety Engineering*, 2006, 23(3): 253-257. (in Chinese).
- [5] YANG Tian-hong, XU Tao, LIU Jian-xin, et al. Coupling model of stress-damage-flow and its application to the investigation of instantaneous seepage mechanism for gas during unloading in coal seam with depth[J]. *Chinese Journal of Rock Mechanics and Engineering*, 2005, 24(16): 2900-2905.
- [6] Cheng Yuanping, Yu Qixiang, Yuan Liang, et al. Experimental research of safe and high-efficient exploitation of coal and pressure relief gas in long distance[J]. *Journal of China University of Mining and Technology*, 2004, 33(2): 132-136. (in Chinese).
- [7] Yu Qixiang, Cheng Yuanping, Jiang Chenglin, et al. Principles and applications of exploitation of coal and pressure relief gas in thick and high-gas seams[J]. *Journal of China University of Mining and Technology*, 2004, 33(2): 127-131. (in Chinese).
- [8] Yuan Liang. Theory of pressure relieved gas extraction and technique system of integrated coal production and gas extraction [J]. *Journal of China Coal Society*, 2009, 34(1): 1-18.
- [9] Yuan Liang, Xue Sheng, Xie Jun. Study on gas content based outburst prediction technologies in China[J]. *Coal Science and Technology*, 2011, 39(3): 47 - 51. (in Chinese).
- [10] Yuan Liang. Key technology for modern mining in Huainan coal[J]. *Journal of China Coal Society*, 2007, 32(1): 8 - 12. (in Chinese).
- [11] Yuan Liang. Gas distribution of the mined-out side and extraction technology of first mined key seam relief-mining in gassy multiseams of low permeability[J]. *Journal of China Coal Society*, 2008, 33(12): 1362 - 1367. (in Chinese).
- [12] Yuan L, Xue S, Xie J. A new system for rapid and accurate determination of gas content in coal[A]. *Proceedings of 23rd World Mining Congress [C]*. Montreal, Canada, 2013: 11 - 15. (in Chinese).
- [13] Yuan Liang. The technique of coal mining and gas extraction by roadway retaining and borehole drilling[J]. *Journal of China Coal Society*, 2008, 33(8): 898 - 902. (in Chinese).
- [14] Yuan Liang, Guo Hua, Shen Baotang, et al. Circular overlying zone at longwall panel for efficient methane capture of multiple coal seams with low permeability[J]. *Journal of China Coal Society*, 2011, 36(3): 357 - 365. (in Chinese).
- [15] Yuan Liang. Key technique to high efficiency and safe mining in highly gassy mining area with complex geologic condition[J]. *Journal of China Coal Society*, 2006, 31(2): 174 - 178. (in Chinese).
- [16] Hu Guozhong, Wang Hongtu, Yuan Zhigang. Discrimination criterion of ultimate gas pressure of protection region for exploiting protective layer[J]. *Journal of China Coal Society*, 2010, 35(7): 1131 - 1136. (in Chinese).
- [17] Xue S, Li X S, Xie J. A new coal sampling system for measurement of gas content in soft coal seams[J]. *Applied Mechanics and Materials*, 2012, 121 - 126: 2459 - 2464. (in Chinese).
- [18] Tian Kunyun, Zhang Jian-guo, LÜ Peng. Probe about the determine method of gas pressure threshold value of coal and gas outburst[J]. *Safety in Coal Mines*, 2012, 43(11): 146-148. (in Chinese).
- [19] Lu Ping, Yuan Liang, Cheng Hua, et al. Theory and experimental studies of enhanced gas drainage in the high-gas face of low permeability coal multi-seams[J]. *Journal of China Coal Society*, 2010, 35(4): 580-585. (in Chinese).
- [20] Hu Qianting, Zou Yinhui, Wen Guangcai, et al. New technology of outburst danger prediction by gas content[J]. *Journal of China Coal Society*, 2007, 32(3): 276 - 280. (in Chinese).
- [21] Li Yaobin, Xue Sheng, Wang Junfeng, et al. Gas diffusion in a cylindrical coal sample-A general solution, approximation and error analyses[J]. *International Journal of Mining Science and Technology*, 2014, 24: 69 - 73. (in Chinese).

Cheng Xia. "The mechanism of protection zone expansion in protected seam with a large-spaced lower protective seam" *International Journal of Modern Engineering Research (IJMER)*, vol. 10(01), 2019, pp 39-48